

<https://doi.org/10.1039/C6TC00264A>
Received 00th January 20xx,
Accepted 00th January 20xx

DOI: 10.1039/x0xx00000x

www.rsc.org/

Croconaines as molecular materials for organic electronics: synthesis, solid state structure and transistor devices[†]

A. Punzi,^a M.A.M Capozzi,^a V. Fino,^a C. Carlucci,^a M. Suriano,^a E. Mesto,^b E. Schingaro,^b E. Orgiu,^c S. Bonacchi,^c T. Leydecker,^c P. Samorì,^c R. Musio,^a G.M. Farinola^{*a}

A series of indolenine-based croconaines has been synthesized and their molecular structure has been investigated together with their solid state organization. Ambipolar semiconducting properties have been demonstrated in thin-film transistors, suggesting croconaines as a new class of molecular materials for organic electronics.

Introduction

Croconaines are interesting molecules based on the croconic acid five-member ring. They can be easily synthesized *via* a one-pot condensation reaction of croconic acid with electron-rich aromatic and heteroaromatic compounds or heterocyclic methylene bases,¹ yielding donor-acceptor-donor type zwitterionic compounds, quite similar to the well-known squaraines. The stronger electron-withdrawing character of the croconic acid moiety with respect to the squaric acid part produces a shift of about 100 nm in their absorption spectrum as compared with those of the corresponding squaraines.^{1e,2} In fact, croconaines exhibit narrow and intense absorption bands in the near-infrared (NIR) region, that can be tuned by varying the donor moieties conjugated with the croconium acid core^{1c,d,e} as well as by introducing substituents on a given donor moiety.^{1b,d,3} This property, combined with high molar extinction coefficients ($10^5 \text{ M}^{-1}\text{cm}^{-1}$), good photostability and strong solvatochromism^{1a,e} have attracted considerable interest towards this class of molecules as effective infrared absorbing dyes. Based on these properties, also pointed out by theoretical studies,⁴ some works on their application^{2,3,5-7} as NIR absorbers have been reported so far, despite their low solubility in both organic solvents and aqueous environment, that hampers their wide use.^{1b,d,5} Recently, thiophene-functionalised croconaine dyes encapsulated in rotaxanes have been reported as efficient photothermal systems.⁶

Incorporation in polymers to form plastic NIR attenuating filters was also reported.⁸ Besides NIR absorption, other intriguing features have been demonstrated in croconaines, including acidochromic³ and ionochromic^{1b,2,7} behavior, useful for application in optical sensors, and third-order nonlinear optical properties for potential ultrafast optical devices.⁹ Light harvesting properties have been investigated for applications in dye-sensitized solar cells, but the recorded efficiencies are discouragingly low (PCE < 0.1%).⁵ No study has been reported so far on solid-state structure and electronic properties of croconaines for use in organic electronic devices.

Here, we report the synthesis and characterization of a series of indolenine-based croconaines, bearing different substituents on the donor moieties. Results of structural investigations in solution by DFT calculations and NMR spectroscopy, and in crystals by Single Crystal X-Ray Diffraction (SCXRD) are presented that shed light on their molecular organization in the solid state. We show for the first time the semiconductive properties of croconaines employed as an ambipolar active layer in organic thin-film transistors. The ambipolar behavior stems from the low band-gap of the molecules, the charge separation within the croconic moiety and also from the favorable energy level alignment at the metal-electrode interface. Our pilot study lays the groundwork for possible applications of croconaine molecules in optoelectronics and sensors.

Results and Discussion

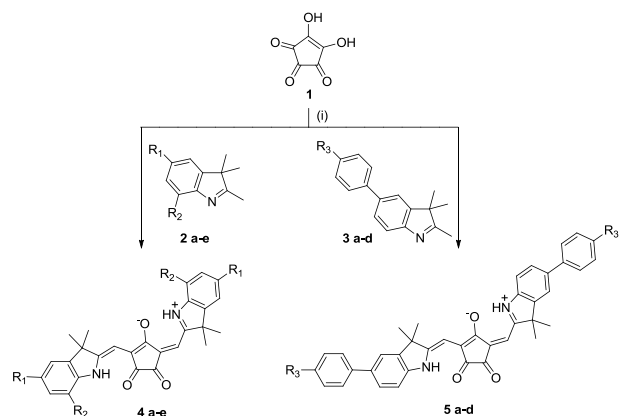
Condensation of croconic acid **1** with indolenines **2** and **3** (scheme 1), yields the corresponding croconaines (Table 1). The UV-Vis absorption spectra in chloroform solution of **4** and **5** are reported in Figure 1. All the croconaine dyes synthesized show quite similar absorption profiles with intense absorption maxima in the NIR region and high molar extinction coefficients (Table 2). The increase in the maximum wavelength for dyes **5** compared to **4** can be attributed to their more extended conjugated system. Among the substituted dyes, compounds **4b,c** and **5b,c** exhibit a maximum wavelength slightly red-shifted with respect to the unsubstituted derivatives **4a**³ and **5a**, respectively.

^a Dipartimento di Chimica, Università degli studi di Bari "Aldo Moro", via Orabona 4, 70126 Bari, Italy. E-mail: gianluca.maria.farinola@uniba.it.

^b Dipartimento di Scienza della Terra e Geoambientali, Università degli Studi "Aldo Moro", via Orabona 4, 70126 Bari, Italy.

^c ISIS & iCFRC, Université de Strasbourg & CNRS, 8 allée Gaspard Monge, 67000 Strasbourg, France.

[†] Electronic Supplementary Information (ESI) available: Synthetic procedures, structural analysis and computational details. See DOI: 10.1039/x0xx00000x



Scheme 1. Synthesis of the croconaines **4 a-e** and **5 a-d**: (i) toluene and 1-butanol, 110 °C, 3h.

Table 1. Yields of croconaines.

Entry	R ₁	R ₂	R ₃	Indolenine	Croconaine (Yield%)
1	H	H		2a [a]	4a (60)
2	Br	H		2b	4b (80)
3	I	H		2c	4c (47)
4	F	H		2d	4d (55)
5	H	F		2e	4e (49)
6			H	3a	5a (60)
7			CH ₃ O	3b	5b (80)
8			C ₆ H ₅ O	3c	5c (47)
9			NO ₂	3d	5d (87)

[a] commercially available

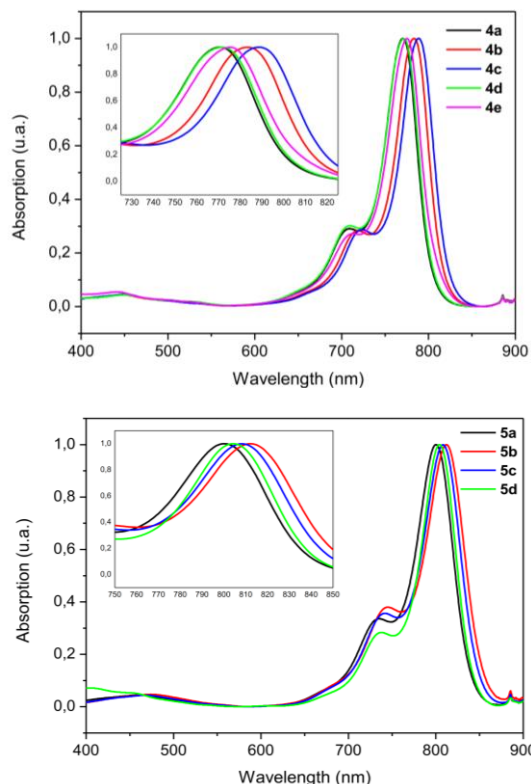


Figure 1. Absorption spectra of compounds **4 a-e** (top) and **5 a-d** (bottom).

Table 2. Photophysical properties of croconaines recorded in CHCl₃ solution.

Croconaine dye	λ_{max} (nm)	λ_{onset} (nm)	ϵ (M ⁻¹ cm ⁻¹)	E_g^{opt} (eV) [a]
4a	770	802	1.92×10^5	1.55
4b	784	814	1.85×10^5	1.52
4c	788	813	1.88×10^5	1.52
4d	771	803	2.23×10^5	1.54
4e	775	808	2.79×10^5	1.53
5a	800	838	2.78×10^5	1.48
5b	812	853	4.18×10^5	1.45
5c	808	847	3.63×10^5	1.46
5d	802	841	1.77×10^5	1.47

[a] E_g^{opt} was estimated from absorption onset wavelengths ($E_g^{\text{opt}} = 1240/\lambda_{\text{onset}}$ (eV)).

The HOMO-LUMO energy levels of croconaines **4** and **5** were determined from cyclic voltammograms, which exhibit two reversible reduction and two quasi-reversible oxidation waves (ESI). As shown in Table 3, the electrochemical properties of croconaines **4** and **5** are very similar, thus suggesting that the structural variations of the indolenine moieties minimally affects their electronic behavior in solution.

Emission quantum yield of **4a** and **4b** in chloroform solution determined by optically matched solutions with **IR-140** as the standard (Φ in EtOH = 0.167) shows very low values (**4a** Φ_{fl} ¹¹ = 0.035; **4b** Φ_{fl} ¹¹ = 0.028).

A PhotoElectron Yield counter operating in Ambient conditions (PEYA) was used to quantify the ionization energy of solution casted thin films of compounds **4a** and **4b**. The ionization energy (IE) levels (HOMO) were assigned at (5.53±0.05) eV and (5.64±0.05) eV for compound **4a** and **4b**, respectively. The IE difference between the two compounds with respect to the vacuum level is consistent with that of the oxidation potential determined by means of CV.

DFT calculations were performed on the model compound **4a** using the B3PW91 functional with the 6-311G(d,p) basis set, both in vacuo and in CHCl₃ solution (by IEF-PCM). Only data in solution are reported. Both in vacuo and in solution the croconaine molecules are planar and exhibit conformational isomerism (Fig. 2).

Table 3. Electrochemical properties of croconaines.

Croconaine	E_{ox} (V) [a]	E_{red} (V) [b]	LUMO (eV) [c]	HOMO (eV) [d]	E_g (eV) [e]
4a	0.15	-1.15	-3.95	-5.25	1.30
4b	0.23	-1.07	-4.03	-5.33	1.30
4c	0.22	-1.07	-4.03	-5.22	1.29
4d	0.18	-1.14	-3.96	-5.28	1.32
4e	0.24	-1.07	-4.03	-5.34	1.31
5a	0.15	-1.12	-3.98	-5.25	1.27
5b	0.13	-1.14	-3.96	-5.23	1.27
5c	0.16	-1.12	-3.98	-5.26	1.28
5d	0.22	-1.05	-4.05	-5.32	1.27

[a] E_{ox} and [b] E_{red} are the average values between the peak potential and the related reverse one measured for the compounds in DCM solution (10⁻³ M) vs Fc/Fc⁺ reference. [c] LUMO and [d] HOMO energy levels were estimated by empirical equations: LUMO = -e(E_{red} + 5.1 V) and HOMO = -e(E_{ox} + 5.1 V).¹⁰ [e] Energy gap was measured as difference between E_{ox} and E_{red} values.

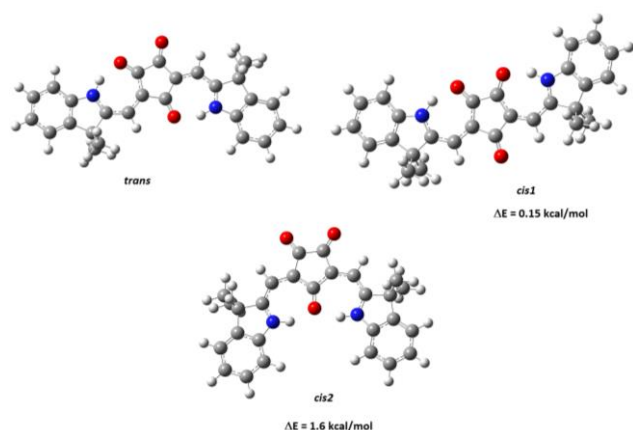


Figure 2. Most stable conformational isomers of **4a**, calculated in CHCl_3 solution at IEF-PCM/B3PW91/6-311G(d,p) level of approximation. The calculated energy differences between the *cis1* / *cis2* isomers with respect to the *trans* isomers are reported.

Compound **4a** can assume three conformations, two symmetric, with the two nitrogen atoms on the same side of the molecule (*cis1* and *cis2*) and one asymmetric conformation with the N atoms opposite with respect to the molecular barycenter (*trans*). Each conformer is stabilized by the formation of two $\text{N-H}\cdots\text{O}=\text{C}$ H-bonds (ESI). For the *trans* conformation these H bonds involve two different carbonyl oxygens, in *cis1* they involve the two symmetric carbonyl groups while in the *cis2* they take place with the same carbonyl group. Different hydrogen bonds are characterized by different geometry and energy. The *trans* isomer is the most stable, but the energy differences calculated between the *cis1* / *cis2* and the *trans* isomers are small (Fig.2). Due to the extended π -delocalization, the interconversion energy barrier is very high and the three isomers are in very slow exchange, as suggested by the ^1H NMR spectrum of **4a** in CDCl_3 (Fig. 3). Four signals are evident in the region of NH, which can be tentatively assigned on the basis of their integral values and of the theoretical calculations results. The less intense signal at 14.61 ppm can be assigned to the two equivalent protons of the *cis2* isomer, the signals at 14.43 and 15.67 ppm to the unsymmetrical *trans* isomer and finally, the signal at 15.07 ppm at the two equivalent protons of the symmetric *cis1* conformer. From the integral values, the ratio of the three conformers in CDCl_3 solution *trans*:*cis1*:*cis2* is 67:30:3.

In addition, Natural Population Analysis was performed on the optimized geometries of the three conformers both *in vacuo* and in CHCl_3 solution. The values of the atomic charges not only confirm the zwitterionic character of croconaines, but also suggest that the charge separation is predominantly localized on the croconic ring molecular core. In fact, in all conformations the three $\text{C}=\text{O}$ bonds are strongly polarized: oxygen atoms bear a significant negative charge, in the range -0.599 to -0.697, whereas calculated charges for carbon atoms are in the range +0.424 to +0.468. The remaining two carbon atoms have a low negative charge (-0.120).¹² According to our preliminary calculations, this charge distribution does not seem to be significantly influenced by the structure of the indolenine moiety.

The crystal structures of **4a** and **4b** were determined by Single Crystal X-Ray Diffraction (SCXRD).¹³ The **4a** crystal belongs to the space group $P\bar{1}$, whereas the **4b** molecule crystallizes in the $P2_1/n$

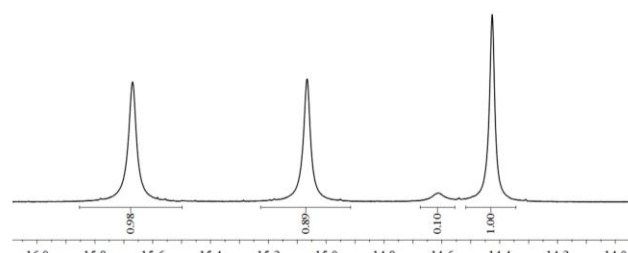


Figure 3. ^1H NMR spectrum of **4a** acquired at 400 MHz in CDCl_3 at room temperature. Expansion of the N-H region.

space group (ESI). X-ray analysis confirms that molecules are essentially planar with the π system delocalized over the whole molecule (Fig. 4). The molecular packing is characterized by parallel sheets linked by π - π stacking and, as suggested by the calculated charge distribution, by electrostatic interactions that involve mainly the croconic ring molecular cores. Specifically, the **4a** packing is dominated by interactions between the π systems of the croconic ring molecular core and one phenyl ring of an adjacent molecule (ESI). For **4b** (Fig. 5) relevant interactions are found between adjacent C1-O1 centrosymmetric equivalent carbonyl groups (electrostatic interactions) with an interatomic distance of 3.082(6) Å, and between π systems of $\text{O}=\text{C}-\text{C}=\text{C}$ fragments and aromatic rings. The distance between the centroids of the π -systems involved is 3.598(6) which is shorter than what reported for squaraine derivatives.¹² Other less strong non-classical H-bonding characterizes the crystal packing of both compounds (ESI). In all the crystals isolated the molecules exhibit a *trans* arrangement with formation of two different intramolecular H-bonds $\text{N-H}\cdots\text{O}=\text{C}$, i.e. $\text{N1-H11}\cdots\text{O3}$ and $\text{N2-H21}\cdots\text{O2}$ (Fig.4).

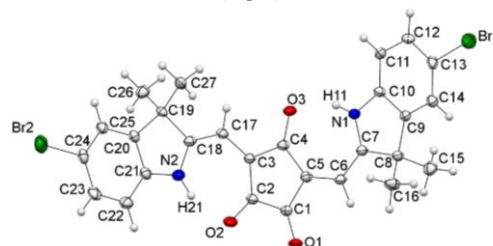


Figure 4. X-ray structure of **4b**.

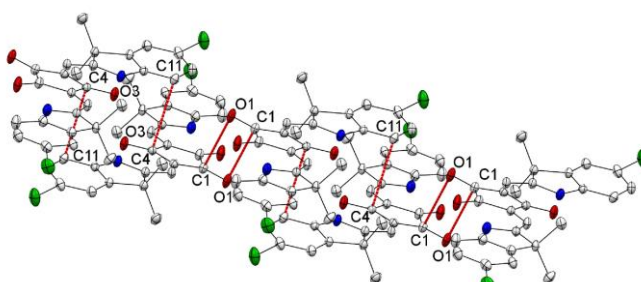


Figure 5. The crystal packing of **4b**. Interactions between carbonyls are indicated by red dashed lines.

The charge transport properties of **4a** and **4b** were tested in bottom-contact bottom-gate transistor devices with Au source and drain electrodes. The active layer was deposited by spin coating from chloroform solution (5 mg/mL) at room temperature. The electrical characterization revealed that both compounds exhibit (i) text-book like output curves (Figures 6a and 6c) and (ii) ambipolar

behavior as highlighted in Figures 6b and 6d. The saturation hole ($\mu_{\text{sat},p}$) and electron ($\mu_{\text{sat},n}$) mobilities determined over 16 devices were found to be balanced and amount to 1) $\mu_{\text{sat},p} = (2.3 \pm 0.3) \times 10^{-5} \text{ cm}^2 \text{ V}^{-1} \text{ s}^{-1}$ and $\mu_{\text{sat},n} = (3.8 \pm 0.1) \times 10^{-6} \text{ cm}^2 \text{ V}^{-1} \text{ s}^{-1}$ for compound **4a** and 2) $\mu_{\text{sat},p} = (2.3 \pm 0.5) \times 10^{-5} \text{ cm}^2 \text{ V}^{-1} \text{ s}^{-1}$ and $\mu_{\text{sat},n} = (3 \pm 1) \times 10^{-6} \text{ cm}^2 \text{ V}^{-1} \text{ s}^{-1}$ for compound **4b**. The $I_{\text{ON}}/I_{\text{OFF}}$ is between 10^4 and 10^5 , revealing an excellent switching ability of the devices. Further, the threshold voltage values were found to be $V_{\text{th},n} = -18 \text{ V}$ and $V_{\text{th},p} = +25 \text{ V}$ for **4a** and $V_{\text{th},n} = -21 \text{ V}$ and $V_{\text{th},p} = +25 \text{ V}$ for **4b**. The large voltage window, $|V_{\text{th},n} - V_{\text{th},p}|$, of approximately 45 V ensures reliable employment of such devices for logic inverters which are the essential elements in all electronic circuits. We believe that the ambipolar behavior observed in such derivatives may stem from both the strong charge separation within the croconic moiety, as demonstrated by DFT calculations, but also from the small bandgap of the dyes and a favorable energy level alignment of HOMO and LUMO with respect to the injecting Au electrode, whose work function amounts to $(4.8 \pm 0.1) \text{ eV}$, which falls within the bandgap of **4a** and **4b**.

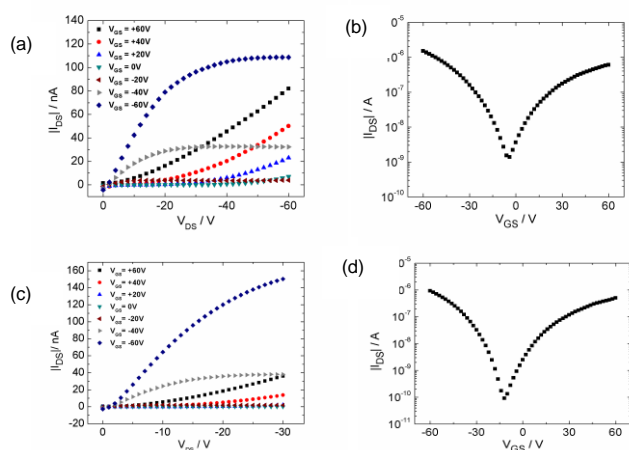


Figure 6. Output (a) and transfer (b) characteristics of compound **4a**. Output (c) and transfer (d) characteristics of compound **4b**. [$W = 10 \text{ mm}$, $L = 20 \text{ }\mu\text{m}$] [$V_{\text{DS}} = -30 \text{ V}$ in the transfer curves]

Conclusions

We have reported a series of indolenine-based croconaines, together with their spectroscopic and electronic properties determined both by electrochemistry and PEYA measurements. An in-depth structural investigation both in solution and in the solid-state has been performed. It reveals a solid-state packing characterized by parallel sheets linked by electrostatic and π - π stacking interactions, resulting in an extended π -conjugation favouring charge transport for both electrons and holes. For the first time the charge transport properties of the croconaine derivatives have been explored. Three-terminal device measurements endorse croconaines as a novel and promising family of small molecules with great potential for the realization of single component complementary-MOS circuitry for flexible, large-area and low-cost electronics. This is an extremely interesting observation, especially considering the very simple and general synthetic protocol, that can in principle be extended to a wide variety of structures with tuneable optical and electronic properties. In addition, the use of ambipolar croconaine derivatives

as semiconducting materials in light-sensing organic FETs paves the way for the realization of large-area and low-cost near-IR sensor arrays.

In conclusion, our work discloses a low cost and versatile novel class of molecules for organic electronics. Further investigations are desirable to both increase charge mobility as well as to extend the number of molecular architectures accessible, with possible applications in molecular electronics.

Acknowledgements

This work was financially supported by Italian Ministero dell'Istruzione, dell'Università e della Ricerca (MIUR), "Project PON02_00563_3316357 (PON MAAT)", Project PON03PE_00004_1 (PON MAIND) and, together with Università degli Studi di Bari "Aldo Moro", Project PRIN 2012 prot. 2012A4Z2RY". PS acknowledges the EC through the ERC project SUPRAFUNCTION (GA-257305), the Agence Nationale de la Recherche through the LabEx CSC (ANR-10-LABX-0026_CSC) and the International Center for Frontier Research in Chemistry (icFRC). SB thanks the EC Marie Curie - IEF fellowship GALACTIC (PIEF-GA-2013-628563).

Notes and references

- 1 a) V. Kurdiukova, A. V. Kulinich and A. A. Ishchenko, *New J. Chem.*, 2012, **36**, 1564; b) R. R. Avirah, K. Jyothish and D. Ramaiah, *J. Org. Chem.*, 2008, **73**, 274; c) T. P. Simard, J. H. Yu, J. M. Zebrowski-Young, N. F. Haley and M. R. Detty, *J. Org. Chem.*, 2000, **65**, 2236; d) D. Keil, H. Hartmann and C. Reichardt, *Liebigs Ann. Chem.*, 1993, 935; e) S. Yasui, M. Matsuoka and T. Kitao, *Dyes Pigm.* 1988, **10**, 13.
- 2 X. Zhang, C. Li, X. Cheng, X. Wang and B. Zhang, *Sensor Actuat. B-Chem.*, 2008, **129**, 152.
- 3 a) M. Puyol, C. Encinas, L. Rivera, S. Miltsov and J. Alonso, *Dyes Pigm.*, 2007, **73**, 383; b) C. Encinas, E. Otazo, L. Rivera, S. Miltsov and J. Alonso, *Tetrahedron Lett.*, 2002, **43**, 8391.
- 4 a) A. Puyad, Ch.R. Kumar and K. Bhanuprakash, *J. Chem. Sci.*, 2012, **124**, 301; b) J. Fabian and R. Peichert, *J. Phys. Org. Chem.*, 2010, **23**, 1137; c) A. Thomas, K. Srinivas, Ch. Prabhakar, K. Bhanuprakash and V. J. Rao, *Chem. Phys. Lett.*, 2008, **454**, 36; d) K. Srinivas, Ch. Prabhakar, C. L. Devi, K. Yesudas, K. Bhanuprakash and V. J. Rao, *J. Phys. Chem. A*, 2007, **111**, 3378; e) Ch. Prabhakar, K. Yesudas, G. K. Chaitanya, S. Sitha, K. Bhanuprakash and V. J. Rao, *J. Phys. Chem. A*, 2005, **109**, 8604; f) Ch. Prabhakar, G. K. Chaitanya, S. Sitha, K. Bhanuprakash and V. J. Rao, *J. Phys. Chem. A*, 2005, **109**, 2614.
- 5 K. Takechi, P. V. Kamat, R. R. Avirah, K. Jyothish and D. Ramaiah, *Chem. Mater.*, 2008, **20**, 265.
- 6 a) G. T. Spence, S. S. Lo, C. Ke, H. Destecroix, A. P. Davis, G. V. Hartland and B. D. Smith, *Chem. Eur. J.*, 2014, **20**, 12628; b) G. T. Spence, G. V. Hartland and B. D. Smith, *Chem. Sci.*, 2013, **4**, 4240.
- 7 S. Wang, T. Cong, Q. Liang, Z. Li and S. Xu, *Tetrahedron*, 2015, **71**, 5478.
- 8 X. Song and J. W. Foley, *Dyes Pigm.*, 2008, **78**, 60.
- 9 Z. Li, Z.-hui Jin, K. Kasatani and H. Okamoto, *Physica B*, 2006, **382**, 229.

- 10 C. M. Cardona, W. Li, A. E. Kaifer, D. Stockdale and G. C. Bazan, *Adv. Mater.*, 2011, **23**, 2367.
- 11 K. Rurack and M. Spieles, *Anal. Chem.*, 2011, **83**, 1232.
- 12 P. H. Wöbkenberg, J. G. Labram, J.-M. Swiecicki, K. Parkhomenko, D. Sredojevic, J.-P. Gisselbrecht, D. M. de Leeuw, D. D. C. Bradley, J.-P. Djukic and T. D. Anthopoulos, *J. Mater. Chem.*, 2010, **20**, 3673.
- 13 Complete crystallographic data are available upon request from the Cambridge Crystallographic Data Centre (12 Union Road, Cambridge, CB2 1EZ, UK; email: deposit@ccdc.cam.ac.uk), by quoting the depository numbers CCDC-1433186 (**4b**), CCDC- 1433187 (**4a**).